

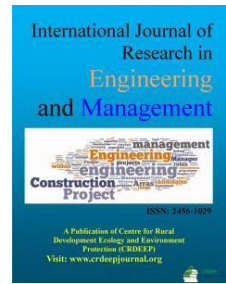
Vol. 4. No. 2. 2020

©Copyright by CRDEEP Journals. All Rights Reserved.

Contents available at:

[www.crdeepjournal.org](http://www.crdeepjournal.org)

International Journal of Research in Engineering &amp; Management (ISSN: 2456-1029)(SJIF: 2.228)

**Full Length Research Paper****Effect of Steel Fiber Ratio and various Reinforcement Ratios on Flexural behavior of HSC& UHSC beams**Mina Nabil<sup>1</sup>, Ezz-Eldin Mostafa<sup>2</sup>, Amr Zaher<sup>3</sup><sup>1</sup>Ph.D. Student at Department of Structural Engineering, Ain Shams University, Cairo, Egypt.<sup>2,3</sup>Department of Structural Engineering, Ain Shams University, Cairo, Egypt.**ARTICLE INFORMATION****Corresponding Author :**

Mina Nabil Malak Henen

**Article history**

Received: 27-12-2020

Revised: 29-12-2020

Accepted: 31-12-2020

**Keywords:**

Ultra-high strength concrete, flexural behavior, vertical deflection

**ABSTRACT**

The main objectives of this research addressed through the experimental work described in this chapter. The main objective is to study the flexural behavior of ultra-high strength concrete beams subjected to concentrated loads. The program incorporated two phases in which specimens were designed and cast to study the desired properties. The first phase reviews a detailed tested specimen. While the second phase deals with the characteristics of the used material, mix proportions, preparation of specimens and loading system. In the current research, eight reinforced UHSC beams were cast and statically tested under the effect of two vertical concentrated loads up to failure at the reinforced concrete laboratory of housing and building research center to investigate the modes of failure, the ultimate load carrying capacity and the flexural behavior of UHSC concrete. The deformation, vertical deflection, concrete strain, longitudinal compression steel strain and tension steel strain were measured. The observed parameters and the description of the specimens and reinforcement in current work will be discussed later.

**Introduction**

Ultra High Strength Concrete (UHSC) is a new advanced concrete that has been transferred from laboratory research to practical applications. Based on the latest developments in concrete technology, UHSC is characterized by extra ordinary mechanical properties (high compressive and tensile strengths & high young's modulus) and has excellent durability properties. Up till now, the use of UHSC is very limited due to its unknown properties that differ from normal strength or high strength concrete. Moreover, the very low ductility of UHSC leads to brittle failure of members produced from it. The deformation behavior of the ultra-high strength matrix in comparison to normal Strength concrete is a contrary matter. Ultra High Strength Concrete (UHSC) with a high compressive strength and an improved durability marks a quantum leap in concrete technology. This high-performance material offers a variety of interesting applications. It allows the construction of sustainable and economic buildings with an extraordinary slim design. Its high strength makes it a suitable building material for bridge decks, storage halls, thin-wall shell structures and highly loaded columns. A new formulation approach by using ultra-fines materials supported by strong development of new admixtures open the way over the last twenty years to amazing progresses in

concrete technology. The ranges of performances and characteristics that are today covered by concrete have been expanded in various directions from ordinary concrete up to ultra-high-performance concrete.

Ultra-High-Performance Concrete (UHPC) is a new class of concrete that has been developed in recent decades. When compared with high performance concrete (HPC), UHPC tends to exhibit superior properties such as advanced strength, durability, and long-term stability. The production of ultra-high strength concrete (UHSC) has been researched in the 1970s. Compressed cement paste achieved a compressive strength of 65 N/mm<sup>2</sup> under heat curing conditions. Intensive research on high performance concrete enhances the knowledge about the use of chemical and mineral admixture in concrete. On this basis a new concrete with a compressive strength of more than 180 N/mm<sup>2</sup> was developed at the beginning of the 1990s in France and Canada with the elimination of coarse aggregate. Higher strength offers savings in material. Weight, or the structural dead load, is a major loading in the design of structures. Consequently, higher strength usually gives us two advantages: less material and less weight. The reduction in weight in turn reduces the demand on material because it reduces the load the structure must carry.

With strength of 200 MPa, the UHPC is almost like steel except its tensile capacity is still comparatively low so it cannot be used like steel. However, this is many folds higher than the regular concrete, the strength of which is around 50 MPa.

**The Experimental program**

**Objective of the Experimental Program**

The main objective of this study is to investigate flexural behavior of Ultra High Strength Concrete (UHSC) Beams. The various specific objectives are:

1. Studying the flexural behavior of UHSC beams.
2. Investigate to optimum minimum reinforcement ratio with minimum crack width UHSC beams.
3. Investigate the effect of steel fiber and various reinforcement ratio on HSC&UHSC beams.
4. Recommendations for ECP for UHSC.

**Details of Test Specimens**

The experimental program was conducted on twelve UHSC concrete beams. All beams with total span 3400 mm were simply supported with 3000 mm clear span, 200 mm projection at each end as shown as Figure.1 and tested beams detailed at Table.1

**Table.1:** Details of specimens.

**The first group:** consists of three specimens with cross section dimensions 100 mm wide and 250 mm height. The lower longitudinal steel reinforcement consists of 3Ø10 with reinforcement ratio 1%, while the upper longitudinal steel reinforcement consists of 2Ø10. The transverse reinforcement consists of closed stirrups 8 mm diameter @100 mm (2-branches) the compressive strength of cubes is 60 Mpa, for the first two specimens and 80Mpa for the third one. The concrete mix for the first specimen is without fiber reinforcement, while the other two specimens have fiber reinforcement with 1% percentage

**The second group:** consists of five specimens with cross section dimensions 100 mm wide and 250 mm height. The low longitudinal steel reinforcement with various reinforcement ratios is (0.7%, 1%, 1.4%, 1.8%, and 2.2%), while the upper longitudinal steel reinforcement consists of 2Ø10. The transverse reinforcement consists of closed stirrups 8 mm diameter @100 mm (2-branches) the compressive strength of cubes is 120 Mpa. The concrete mix for all specimens is with 1% fiber reinforcement

Groups	Specimens	$V_f$ %	Main Steel	$P_{sv}$ %	$F_{cu}$	$b*t(mm)$
The First Group	60WF25-1%	0%	3 $\phi$ 10	1%	60	10*25
	60BF25-1%	1%	3 $\phi$ 10	1%	60	10*25
	80BF25-1%	1%	3 $\phi$ 10	1%	80	10*25
The Second Group	120UH25-0.7%	1%	2 $\phi$ 10	0.7%	120	10*25
	120UH25-1%	1%	3 $\phi$ 10	1%	120	10*25
	120UH25-1.4%	1%	4 $\phi$ 10	1.4%	120	10*25
	120UH25-1.8%	1%	5 $\phi$ 10	1.8%	120	10*25
	120UH25-2.2%	1%	6 $\phi$ 10	2.2%	120	10*25

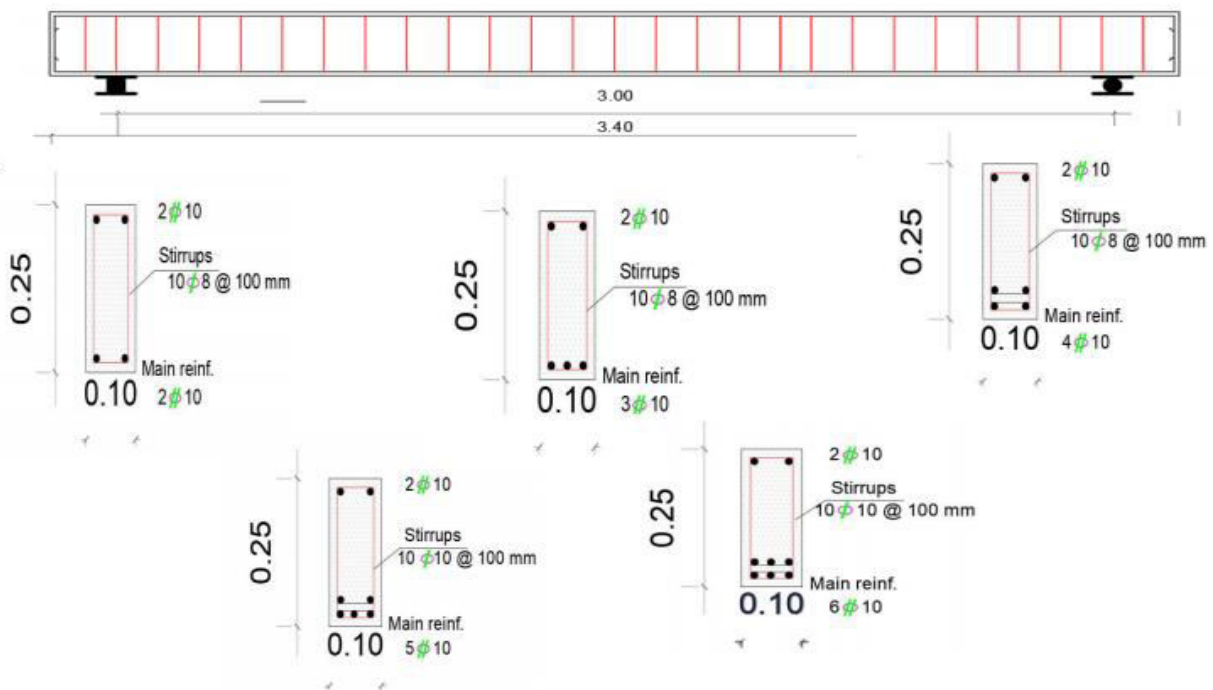


**Fig. 1** Specimen details

**Material properties**

The concrete mix was ordered from a concrete mixing plant with a characteristic concrete strength of 60-80-120 MPa. Two sets of

six concrete cubes and six concrete cylinders were cast alongside the beams, Weighted and tested on the same day of beam testing to ensure the resistance of the required concrete.

**Table.2** Mix proportion of Ultra-High Strength Concrete

Mix	Cement kg/m <sup>3</sup>	S.F. %	Sand /Total agg.		Quartz powder/ Total agg	Coarse aggregate /Total agg.		W/B	Ad %	St Fiber %	Curing
			Siliceous	Quartz		Dolomite	D <sub>5</sub>				
Mix 60	500	10	0.4		0.25	0.6	0.25	0.25	2	1	water
Mix 80	500	18	0.4		0.25	0.6	0.2	0.2	3.5	1	water
Mix 120	800	20	0.25		0.25	0.5	0.16	0.16	4	1	SC-7d

**Experimental results and analysis**

A total of eight beam specimens were tested up to failure. All of them failed in flexural behavior before Shear capacity is reached. A summary of the test results for each tested beam specimens is presented in Table.3, includes the reinforcement ratio, depth to width ratio, moment cracking load, final and crack width, and the failure load.

**CRACKING BEHAVIOR**

Similar characteristics of crack formation were observed for all beams. The crack formation was initiated in the flexural span between the two concentrated loads where the tensile stress is highest and shear stress is zero. the cracks were perpendicular to the direction of the maximum principal tensile stress induced by pure bending, as the load increased, the numbers, and width of cracks had increased.

**Cracking behavior for group I**

- For specimen **60WF25-1%** the specimen had experienced the formation of fine cracks vertically in the middle of beam span between the two-point load the final failure of that specimen was characterized by flexural failure in the mid-span and it were small the initial crack load about 40 KN and have more ductility with medium crack width presented by FIG.2.
- For specimen **60BF25-1%** the specimen had experienced the formation of fine cracks vertically in the middle of beam span between the two-point load he final failure of that specimen was characterized by flexural failure in the mid-span and it were small the initial crack load about 57 KN, the failure load was increased by 34% about **60WF25-1%** have less than ductility and larger crack width from control specimen presented by FIG .3.
- For specimen **80BF25-1%** the specimen had experienced the formation of fine cracks vertically in the middle of beam span between the two-point load he final failure of that specimen was characterized by flexural failure in the mid-span and it were small the initial crack load about 60 KN, the failure load was increased by 40% about **60WF25-1%** have less than

ductility and larger crack width from control specimen presented by FIG.4.

**Cracking behavior for group II**

- For specimen **120UH25-0.7%** the specimen had experienced the formation of fine cracks vertically in the middle of beam span between the two-point load he final failure of that specimen was characterized by flexural failure in the mid-span it were small the initial crack load about 45 KN presented by FIG.5.
- For specimen **120UH25-1%** the specimen had experienced the formation of fine cracks vertically in the middle of beam span between the two-point load he final failure of that specimen was characterized by flexural failure in the mid-span it were small the initial crack load about 60 KN the failure load was increased by 29% about **120UH25-0.7%** presented by FIG.6.
- For specimen **120UH25-1.4%** the specimen had experienced the formation of fine cracks vertically in the middle of beam span between the two-point load he final failure of that specimen was characterized by flexural failure in the mid-span it were small the initial crack load about 75 KN the failure load was increased by 58% about **120UH25-0.7%** presented by FIG.7.
- For specimen **120UH25-1.8%** the specimen had experienced the formation of fine cracks vertically in the middle of beam span between the two-point load he final failure of that specimen was characterized by flexural failure in the mid-span and it were small the initial crack load about 80 KN the failure load was increased by 80% about **120UH25-0.7%** presented by FIG.8.
- For specimen **120UH25-2.2%** the specimen had experienced the formation of fine cracks vertically in the middle of beam span between the two-point load he final failure of that specimen was characterized by flexural failure in the mid-span it were small the initial crack load about 115 KN the failure load was increased by 123% about **120UH25-0.7%** presented by FIG.9.

It was found at sample **120UH25-0.7%** designed with  $A_s$  min by ECP (201) the section had balanced failure because the  $P_{cracking}$  equal the  $P_{ultimate}$  it means that the longitudinal steel wasn't contributed with UHSC at its behavior but when designed at sample **120UH25-1.4%** by 2-times  $A_s$  min by ECP (201) equation it was found the contribution of longitudinal steel was founded  $P_{cracking}$  equal (2/3) the  $P_{ultimate}$ .

**AND.**

According to calculations of  $A_s$  min with  $M_{cr}$  &  $F_{ctr}$  experimentally it was found the main reinforcement ratio covered

the  $M_{cr EXP}$  equal 2-times  $A_s$  min by ECP (201) equation; the sample **120UH25-1.4%** designed by 2-times reinforcement ratio by ECP (201); it was found the  $P_{cracking}$  of sample **120UH25-1.4%** experimentally equal the  $P_{cracking}$  analytically and it both of them equal (2/3) the  $P_{ultimate}$ .

All beams at group II by increased the reinforcement steel ratio increased the ultimate load and decreased the deflection values and crack width values

**Table.3.** Test results summary

Groups	Sample	ACI Design Failure Load (KN)	EXP Failure Load (KN)	P Cracking Fctr exp	$P_{Cracking}$ curves	Final Crack Width (mm)	Max. Deflection At Middle Span (mm)	D/W
Group.1	60WF25-1%	40.5	50	27.5	40	3.26	65	2.5
	60BF25-1%	40.5	67	27.5	57	4.71	57.1	
	80BF25-1%	41.2	70	29	60	3.5	62	
Group.2	120UH25-0.7%	28.2	55	59	45	10	80	
	120UH25-1%	42	71	61.2	60	8	75	
	120UH25-1.4%	55.25	87	62.6	75	6.7	70	
	120UH25-1.8%	68.3	99	64	80	4	50	
	120UH25-2.2%	81	123	66	95	2	35	



**Fig.2** Crack pattern and the failure in specimen 60WF25-1%



**Fig.3** Crack pattern and the failure in specimen 60BF25-1%



**Fig.4 crack pattern and the failure in specimen 80BF25-1%**



**Fig.5 crack pattern and the failure in specimen 120UH25-0.7%**



**Fig.6 crack pattern and the failure in specimen 120UH25-1%**



**Fig.7 crack pattern and the failure in specimen 120UH25-1.4%**



Fig.8 crack pattern and the failure in specimen 120UH25-1.8%



Fig.9 crack pattern and the failure in specimen 120UH25-2.2%

**Crack width**

Crack width of all beams was measured using linear variable displacement transducers (LVDT's) and recorded data using a data acquisition system. The crack width was measured to determine the maximum crack width through the span of each tested beam from zero up to the failure load. The experimental load-crack width curves of the beams are shown in Figures (10) to (12) the values of maximum crack width of beam are shown in Table.3.

• **Load-Crack Width of Group I**

The load-crack width relationship of first group beams showed that the crack width increased with an increase of steel fiber ratio at 60wf25-1% & 60bf25-1% by 30% because the steel fiber increases the capacity of beam and ultimate load

Increasing concrete grade has also great effect on minimizing final crack width. For beams with the same reinforcement and geometric configurations (80BF25-1%,  $F_{cu} = 80\text{MPa}$ ) have lower crack width with 35%, and 26%, respectively compared to (60BF25-1%,  $F_{cu} = 60\text{MPa}$ ) for the load-crack width relationship shown in Figure.10

• **Load-Crack width of Group II**

The load- crack width relationship of second group beams showed that the crack width decreased with an increase of reinforcement steel ratio by 20%, 33%, 60%, and 80% compared to the reference beam (120UH25-0.7%). For the load-crack width relationship shown in Figure.11

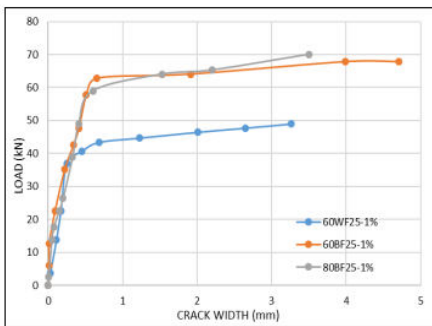


Fig.10 Load –Crack width Curve for Group I

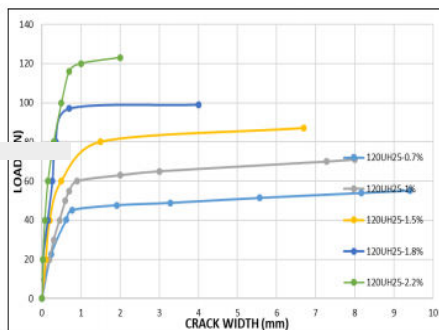


Fig.11 Load –Crack width Curve for Group.II

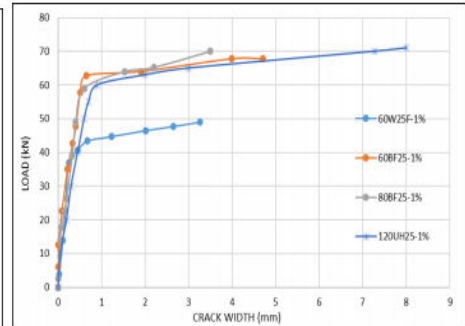


Fig.12 Load –Crack Width Curve for Group. I& Group.II

**Load-deflection response**

Deflection of all beams was measured using linear variable displacement transducers (LVDT's) and recorded data using a data acquisition system. The vertical deformations were measured by three points on each beam and one Point in the mid-span of the beam and other two point at first and last quarter of to predict the deflection shape of the tested beams.

The experimental load-deflection curves at points of maximum deflection of the beams are shown in Figures (13) to (15). The values of maximum deflection of beam are shown in Table.3.

**Load-Deflection Response of Group I**

The load-deflection relationship of first group beams showed that the deflection decreased with an increase of steel fiber ratio at 60wf25-1% & 60bf25-1% by 13% but decreased with increase compressive strength because increased the applied load at 80bf25-1% by 5% For the load-deflection relationship shown in Figure.13

**Load-Deflection Response of Group II**

The load-deflection relationship of second group beams showed that the deflection decreased with an increase of reinforcement steel ratio by 7%, 13%, 38%, and 57%) compared to the reference beam (120UH25-0.7%). For the load-deflection relationship shown in Figure.14

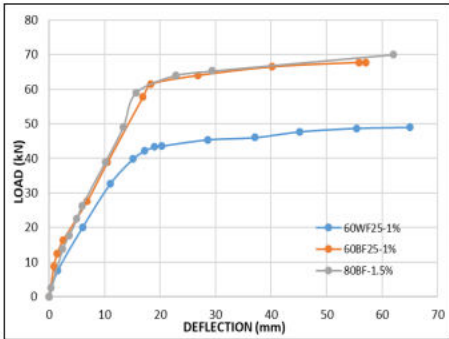


Fig.13 Load –Deflection Curve for Group I

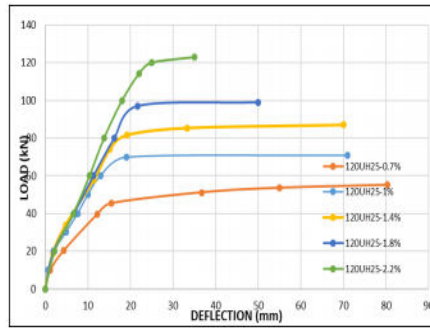


Fig.14 Load –Deflection Curve for Group II

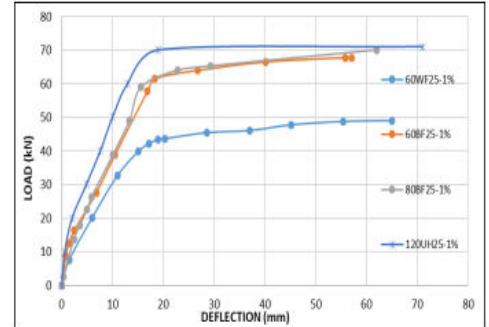


Fig.15 Load –Deflection Curve for Group. I & Group II

strain gauges attached on the top of the concrete surface and horizontally LVDT to measure the concrete strain at the compression zone during testing to ensure that the compression failure doesn't occur during load increment

**Compressive Concrete Strain of Group I**

From comparing the beam 60bf25-1% with steel fiber ratio 1% by volume with the control beam 60wf25-1% it noticed that there is a significant increase in the concrete strain of the beam 60bf25-1% because presence steel fiber which increased the capacity of beam when comparing at the same load of yielding of longitudinal main steel it noticed increase the concrete strain by 400%. From comparing the beam 80bf25-1% with steel fiber ratio 1% by volume and increase the compressive strength with the control beam 60wf25-1% it noticed that there is a significant increase in the concrete strain of the beam 80bf25-1% because presence steel fiber which increased the capacity of beam when

it noticed increase the concrete strain by 270%. From comparing the beam 80bf25-1% with steel fiber ratio 1% by volume and increase the compressive strength with the control beam 60bf25-1% it noticed that there is a significant decreased in the concrete strain of the beam 80bf25-1% because increase the compressive strength which increased the capacity of beam when comparing at the same load of yielding of longitudinal main steel it noticed decreased the concrete strain by 67%. are presented in Figure.16.

**Compressive Concrete Strain of Group II**

The load- concrete strain relationship of second group beams showed that the concrete strain increased with an increase of reinforcement steel ratio at the same load of yielding of longitudinal main steel to reach the max strain at failure =0.004.the value of concrete strain for all beams are constant at ultimate load are presented in Figure.17

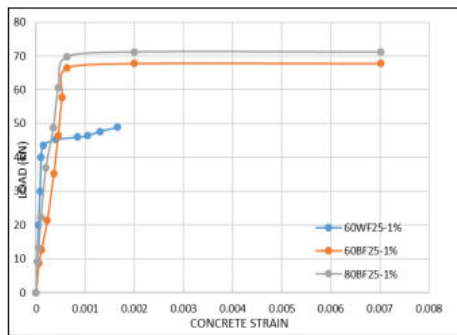


Fig.16 Load –Concrete strain Curve for Group.I

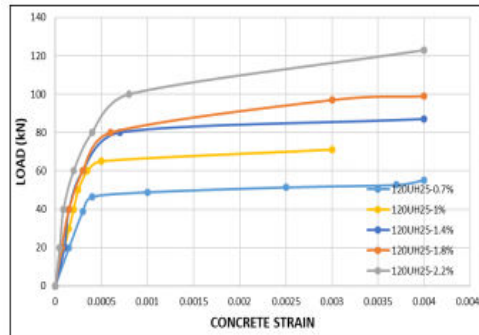


Fig.17 Load –Concrete strain Curve for Group.II

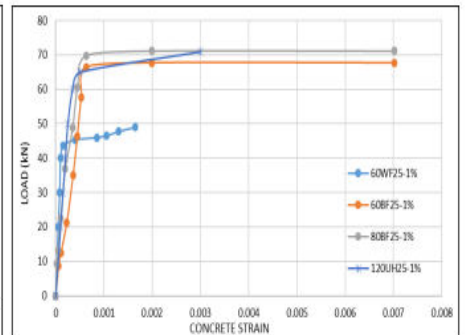


Fig.18 Load –Concrete strain Curve for Group.I & Group.II

**Longitudinal steel strain**

Attached strain gauges at the bottom longitudinal bars were used to measure the steel reinforcement stain during testing process connected to data acquisition system.

**• Longitudinal Steel Strain of Group I**

The load- Longitudinal steel strain relationship of first group beams showed that the Longitudinal steel strain increased with an increase of steel fiber ratio at 60wf25-1% & 60bf25-1% by 30% because the steel fiber increases the capacity of beam and ultimate load. Increasing concrete grade has also great effect on maximize Longitudinal steel strain equally effect of absence steel fiber ratio. For beams with the same reinforcement and geometric configurations (80BF25-1%, Fcu = 80MPa) & (60BF25-1%, Fcu

= 60MPa) have higher Longitudinal steel strain with 62.5% compared to (60WF25-1.5%, Fcu = 60MPa without fiber) For the load-longitudinal steel strain relationship shown in Figure.19

**• Longitudinal Steel Strain of Group II**

The load- Longitudinal Steel Strain relationship of second group beams showed that enhance the longitudinal steel strain by 60% from steel strain by 2-times minimum reinforcement ratio of the ECP for depth to width ratio 2.5 compared to (120UH25-0.7%). For the load-longitudinal steel strain relationship shown in Figure.20.

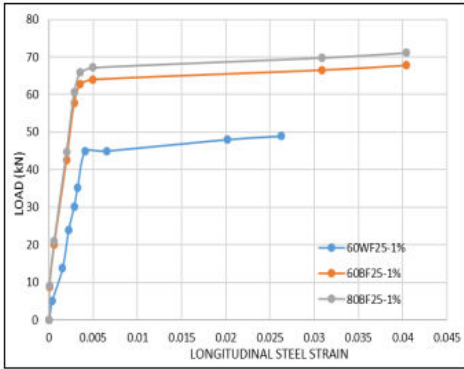


Fig.19 Load –Longitudinal Steel Strain Curve for Group I

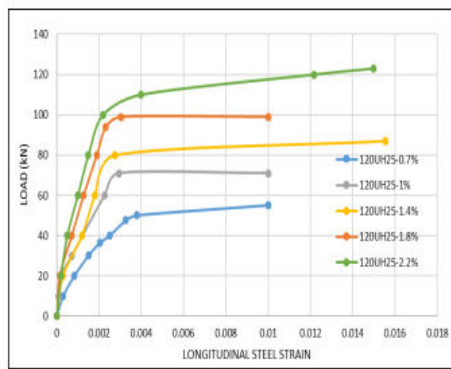


Fig.20 Load – Longitudinal Steel Strain Curve for Group.II

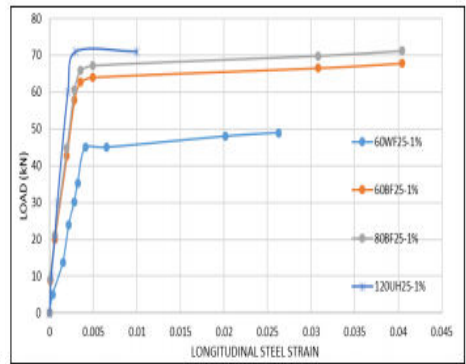


Fig.21 Load – Longitudinal Steel Strain Curve for Group. I&Group.II

**Conclusion**

- 1- The experiments show that producing UHSC with desired characteristic compressive of (120 MPa) would only be achieved by selecting the same mix proportions of HSC along with 1% steel fiber by volume. It was also captured that the indirect tensile strength, flexural strength, and modulus of elasticity of UHSC were enhanced with 220%, 217%, and 161%, respectively, over their corresponding values for HSC.
- 2- Generally, the increase in the characteristic strength of concrete works on decreasing the section ductility. It is however, in the current research adding 1% fiber enhanced the ductility of the examined beams significantly. For example, Beam (120UH25-1%) with (Fcu=120 MPa) reached almost the same ductility index as beam (60WF25-1%) with (Fcu = 60 MPa) and with no fiber.
- 3- Regarding HSC beams, for group (G1), It was noticed the addition of fibers acted on minimizing final beam deflection, and consequently decreased the ductility. Beam (60BF25-1%) with fibers has less deflection than Beam (60WF25-1%) without fiber by 13%.
- 4- Increasing concrete grade has also great effect on minimizing final crack width. For beams with the same reinforcement and geometric configurations (80BF25-1%, Fcu = 80MPa) have lower crack width with 35%, and 26%, respectively compared to (60BF25-1%, Fcu = 60MPa).

- 5- According to calculations it was found the cracking load is equal or more ultimate load for specimens have reinforcement ratio according to ECP it means that the longitudinal tension steel was not contributed with UHSC beam behavior but when increase the value reinforcement ratio of ECP the contribution of the longitudinal tension steel was founded by difference between cracking load equal 2/3 ultimate load.
- 6- For all examined full-scale beams, it was observed that all failure modes were due to pure bending without any signs of shear failure modes. The cracks were generated mainly in the mid-span of the beam and particularly between the two points of load application. For all beams the strain of the tensile reinforcement was beyond the yield value (i.e. greater than 0.0018), simultaneously, the strain of compressive steel was less than or equal to concrete crushing strain (i.e.  $\epsilon_c = 0.003$ ).
- 7- Experimentally, for G2 (Fcu=120 MPa, and same (width: thickness) ratio of (1:2.5)), the achieved ultimate load for beams with different longitudinal tensile reinforcement ratio of (1%, 1.5%, 2%, 2.5%, and 3%) was increased gradually by (29%, 58%, 80%, and 123%), respectively, over the reference beam (UH25-1%). Whereas, the final vertical deflection at mid-span of these beams decreased gradually by (7%, 13%, 38%, and 57%) compared to the reference beam (UH25-1%). Finally, the crack width of the same beams decreased gradually by (20%, 33%, 60%, and 80%), respectively, with reference to beam (UH25-1%).

8- It was found experimentally & analytically that a ratio equal to double the minimum reinforcement percentage stated by ECP (201) can be considered as the minimum ratio for UHSC. It was noted that values lesser the stated could end-up with significant sudden increase in the tensile reinforcement strain as well as unacceptable deflection values. (as abeam 120UH25-1.4%).

9-the 2-times minimum reinforcement ratio of the ECP decreased the crack width about 33% and decrease the deflection by (13%) at 0.003 concrete strain by enhance the longitudinal steel strain by 60% from steel strain by minimum reinforcement ratio of the ECP for depth to width ratio 2.5.

## References

- Hajar Z., Simon A., Lecointre D. and Petitjean J., (2004) "Design and Construction of the World First Ultra-High Performance Road Bridges" Proceedings of the International Symposium on Ultra High Performance Concrete, Kassel, Germany, September 13-15, 2004, pp. 39-48.
- Haleerattanawattana P. and Limsuwan E., (2004) "Strength-Based Gradation of Coarse Aggregates for Ultra-High-Strength Concrete" Proceedings of the International Symposium on Ultra High Performance Concrete, Kassel, Germany, September 13-15, 2004, pp. 239-265.
- Heinz D., Ludwig H. M., (2004) "Heat Treatment and the Risk of DEF Delayed Ettringite Formation in UHPC" Proceedings of the International Symposium on Ultra High Performance Concrete, Kassel, Germany, September 13-15, 2004, pp. 717-730.
- Johansen V. C., Taylor P. C. and Tennis P. D., (2006) "Effect of Cement Characteristics on Concrete Properties" EB226, 2nd edition Portland Cement Association, Skokie, Illinois, USA.
- Kaminska M. E., (2002) "High-Strength Concrete and Steel Interaction in RC Members" Cement & Concrete Composites , Issue No. 2, Vol. 24, pp. 281-295.
- Ma J., (2001) "Experimental Investigation for the Production of Ultra High Strength" LACER, Leipzig Annual Civil Engineering Report, No. 6, pp. 215-228.
- Ma J., Orgass M., Dehn F., Schmidt D. and Tue N. V., (2004) "Comparative Investigations on Ultra-High Performance Concrete with and without Coarse Aggregates", Proceedings of the International Symposium on Ultra High Performance Concrete, Kassel, Germany, September 13-15, pp. 205-212.
- Martirena J. F., Day R. L.Middendorf B., Gehrke M., Martínez L. and Dopico J. M., (2004) "Lime-Pozzolan Binder As A Very Fine Mineral Admixture in Concrete" Proceedings of the International Symposium on Ultra High Performance Concrete, Kassel, Germany, September 13-15, pp. 117-131.
- Orgass M. and Klug Y., (2004) "Steel Fibre Reinforced Ultra-High Strength Concretes" LACER, Leipzig Annual Civil Engineering Report, No. 9.
- Öztaş A., Pala M., Özbay E., Kanca E., çağlar N. and Bhatti M. A., (2006) "Predicting The Compressive Strength and Slump of High Strength Concrete Using Neural Network" Construction & Building Materials Vol. 20, Issue 9., pp 769-775.